12,18

Tunneling current between structural elements of thin graphene/nanotube films

© O.E. Glukhova, M.M. Slepchenkov, P.A. Kolesnichenko

Saratov National Research State University,
Saratov, Russia

E-mail: glukhovaoe@info.sgu.ru

Received July 26, 2021
Revised July 26, 2021
Accepted August 4, 2021

Based on the constructed atomistic models of graphene/nanotube films with different numbers of nanotubes in supercells, we carried out *in silico* studies of the regularities of the nonuniform density distribution, which determine the presence of an island structure in such films. As a result of quantum molecular dynamics modeling, it is found that thin tubes of subnanometer diameter are enveloped in graphene sheets, which makes them energetically stable and stable. We also studied tunneling contacts between individual film fragments that are not covalently bound, in particular, between graphene sheets with different topologies of contacting *zigzag* and *armchair* edges, depending on the distance between them, and between tubes of different chiralities, including (6,3), (4,4), (6,5), (12,6) and (16,0).

It is found that the tunnel contacts of tubes with a semiconductor type of conductivity are characterized by the presence of voltage intervals with a negative differential resistance in the $I-V$ characteristic. Such voltage intervals are not observed at all for tubes with a metallic character of conductivity. The new knowledge obtained is important for assessing the electrical conductivity of such films, two-thirds of which are semiconductor tubes.

Keywords: graphene, nanotubes, tunnel contacts.

DOI: 10.21883/PSS.2022.14.54349.180

1. Introduction

Two-dimensional materials are prospective for use in atomically thin electronics, optoelectronics and flexible electronics due to their controlled electronic properties, optical transparency, easiness of transition onto a substrate and compatibility with modern technologies for integrated circuits [1]. However, thin films with branched structure, created based on single-wall carbon nanotubes (SWCNT) and graphene shells/nanoribbons [2], also have the similar properties. Control of films topology is performed with laser targeted exposure from one side, and from another — synthesis of graphene with molecular even edges was already obtained a decade ago [3–7]. Effect of edge states of graphene nanoribbons is already studied for applications in planar graphene electronics [8]. It is shown, that planar configuration of graphene offers exciting possibilities for building a tunnel field transistor based on it [9]. Many works are dedicated to SWCNT applications. As was repeatedly shown, SWCNT can be used in field transistors [10], in nanochromatography [11], various sensors [12]. At the same time, nanotubes form grids with branched structure. The modern approach to synthesis of grids based on SWCNT and graphene fragments using laser irradiation allows to obtain high-strength and high-conductivity thin films, applied not only in electronics, but also in biomedicine [2]. One of the important issues of such grids application in field transistors is an influence of resistance of tunnel transition between structural elements of the grid and contact electrodes on transistors characteristics. However, even if such grids are not used in transistors, the issue of influence of tunnel transitions, connecting individual fragmental structural elements with each other, on electrical conductivity of the whole nanostructure system, always remains relevant [13,14]. In the work [14], dedicated to tunnel transitions between SWCNT, it was noticed, that for reduction of negative effect of tunnel transitions it is necessary to increase density of films of nanotubes, that, as known, is heterogeneous. Thus, it should be noted, that at synthesis of films of SWCNT and graphene fragments, the film density acquires so called island nature, when there are explicit local regions with increased density in film structure.

This work is dedicated to *in silico* study of the regularities of tunnel current between graphene sheets and chiral SWCNT, that form a thin film with island structure. Tubes of various chirality, particularly, thin tubes (6,3) and (4,4), as well as the most synthesized ones — (6,5), (12,6) and (16,0), were examined.

2. Mathematical modeling: approaches and methods

Green function method and tight-bond approximation were used for tunnel contacts calculations. Within this

formalism, tunnel current is described with expression [15]:

$$I = \frac{e}{h}\int_{-\infty}^{\infty} Tr\left[A_L(1 - t^{\dagger}g_R^{-}tg_L^{-})^{-1}t^{\dagger}A_R t(1 - g_L^{+}t^{\dagger}g_R^{+}t)^{-1}\right] \times [f_L - f_R]d\varepsilon, \quad (1)$$

where $g_{R,L}^{+} = [(\varepsilon + iO^{+})1 - H_{R,L}]^{-1}$ — retarded Green function for edge atoms of the right (left) contacts, $g_{R,L}^{-} = (g_{R,L}^{+})^{\dagger}$, $A_{R,L} = i(g_{R,L}^{+} - g_{R,L}^{-})$ — spectral density of electrons, t — matrix of interaction of atoms of the left and right contacts, $f_L = f(\varepsilon - eV/2)$, $f_R = f(\varepsilon + eV/2)$, $f(\varepsilon) = [1 + \exp(\varepsilon/k_{\mathrm{B}}T)]^{-1}$ — Fermi–Dirac function.

The described approach is implemented in Mizar software, developed with participation of authors of this work [16]. Both contacting objects are subject to common gate influence. System reaction to gate voltage was accounted the regular way: $H_{R,L}(\varepsilon) \to H_{R,L}(\varepsilon + V_g)$. It should be noted, that the second summands in parentheses of expression (1) consider influence of one contact on electron states of another. Earlier in the work [17] the apparatus of Green function was used combined with pi-electron approximation for studying the tunnel contacts between graphene sheets with the same topology of edges. The high efficiency of the applied approaches was demonstrated. All calculations are performed for $k_{\mathrm{B}}T = 0.001t_0$ and at gate voltage $V_g = 0.05t_0$ (t_0 — parameter of interaction between adjacent atoms [17]).

Building of atomistic models of graphene/nanotube films was performed using self-consistent-charge density-functional tight-binding method (SCC DFTB method), as well as with application of universal force field (UFF) for consideration of Van der Waals interaction of individual film fragments. An equilibrium configuration of thin film supercells was achieved by minimizing the total energy during variation of all film supercell atom coordinates with the corresponding setting of periodic boundary conditions. Then, for obtaining the atomic structure of the films under normal conditions (temperature of 300 K and normal pressure), molecular-dynamic modeling (MDM) was performed for 1 ns with time step of 1 fs. At the same time, the total energy, kinetic energy, supercell volume and other energetic and mechanical parameters were recorded with a step of 1 ps. It should be noted, that during MDM not only atoms coordinates, but also the supercell translational vectors were varied (to obtain their optimal values under normal conditions), resulting in volume change during MDM. All mentioned calculations were performed using DFTB+ software package [18]. This software package, like Mizar, is proved itself as a reliable tool for quantum predictive modeling of new nanostructure properties.

3. Atomistic models of graphene/nanotube films with island structure

Fragments of graphene shells of various size, fragments of mono-bilayer graphene sheets and thin nanotubes with chirality of (4,4) and (6,3) were initially used for building the atomistic models of graphene/nanotube films. As known, thin films can not exist on its own due to energy instability, so they can exist in external tube body or as part of composite structures only. Therefore they were chosen for this model of the film, where tubes are sort of enveloped with graphene sheets and isolated from surrounding.

Figure 1, *a* shows one of the built atomistic models of similar film supercell. Supercell sizes until MDM implementation (see i. 2) were $3.4 \times 4.8 \times 4.0$ nm. Single supercell contains only two tubes (4,4) and (6,3) with atoms number of 4105. During MDM the values of total energy E_{tot} changed with time (Fig. 1, *b*). It may be said, that the energy varied near average value, that was -3121 eV (obtained by averaging over the whole time, i.e. for 1 ns). The system total energy oscillations are causes, from one side, by a thermal energy, and from another — by a process of supercell atomic grid optimization. As seen from Fig. 1, *b*, by the end of the molecular-dynamic modeling, at the 850-th picosecond, the energy oscillations are observed near the value below average one, thus indicating the structure stabilization and achieving its optimal energy-favorable state. Indeed, if during the first 400 ps the energy oscillations of $1-1.5\%$ near the average value are observed, then after 500-th picosecond the oscillations become less than 1%, which is ~ 0.5 ps by absolute value. The similar oscillations are observed for volume value (see Fig. 1, *b*). During the first 300 ps the volume is almost the same, but then the supercell volume increases during MDM, indicating the increase of translation vectors lengths. By the end of modeling the situation stabilizes, and the volume value varies near the average value within $\pm 0.07\%$. The average volume value over MDM time was 71.528 nm^3. It should be noted, that during MDM the translation vectors (i.e. supercell lengths) varied along all thee axes X, Y and Z. Structure, presented in Fig. 1, *a*, corresponds to optimal supercell configuration with sizes of $3.58 \times 5.00 \times 4.00$ nm. From the obtained 3D cell we can form the films with the required thickness. It is seen well, that graphene fragments overlap the tubes, like enveloping them in a cocoons, thus providing the energy stability for thin tubes. Length of tube (4,4) as per results of the cell optimization was ~ 4.7 nm, while of tube (6,3) — 3.26 nm, that is less, than a length of a periodic box along Y axis.

Another model of graphene/nanotube film is presented in Fig. 2, *a*. Its supercell includes two tubes (4,4) and two tubes (6,3). Atomistic structure building technique was the same as in the previous case. This supercell sizes were $4 \times 5 \times 4$ nm before MDM (see section 2), and it includes 4358 atoms. Variations of total energy and volume value of

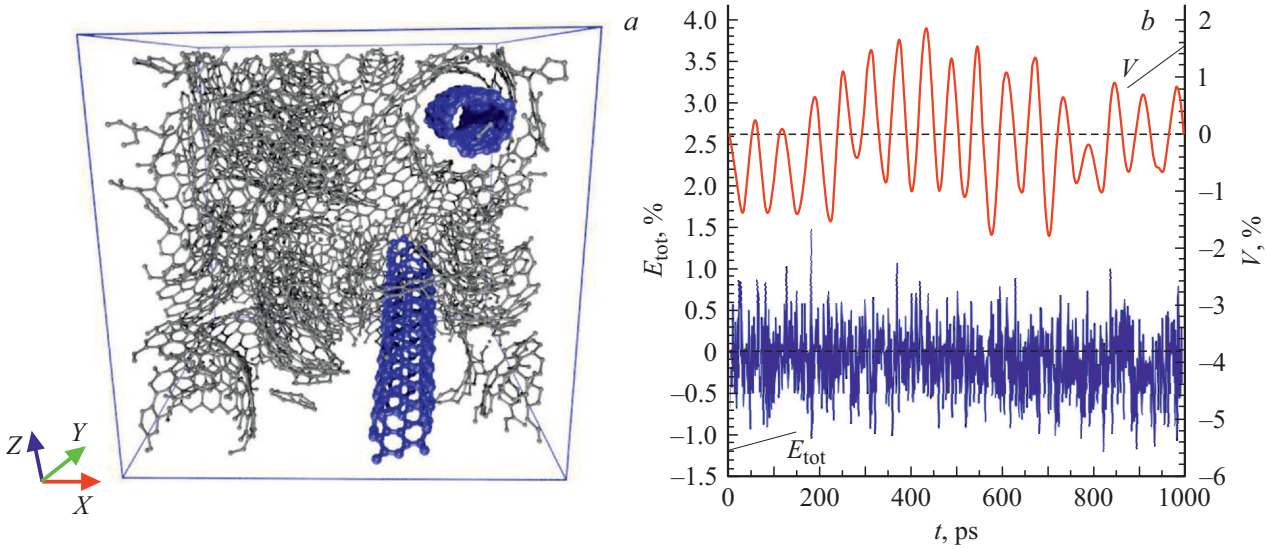

Figure 1. The first model of a film with two tubes in a cell: (*a*) atomistic model of a supercell; (*b*) diagrams of variation of total energy E_{tot} and volume V.

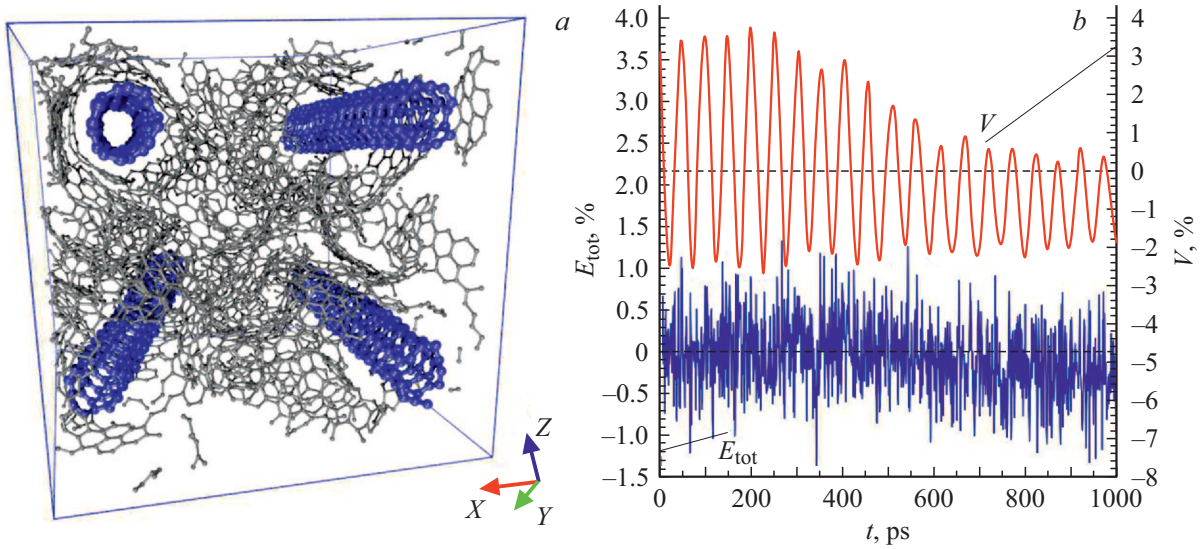

Figure 2. The second model of a film with four tubes in a cell: (*a*) atomistic model of a supercell; (*b*) diagrams of variation of total energy E_{tot} and volume V.

the cell are presented in Fig. 2, *b*. As in the previous option of film model, the total energy reduces in its oscillations near equilibrium position after 700-th picosecond. Its value becomes significantly less than the average one, equal to −3161 eV, while oscillations — less than 0.5%. The same situation is observed in behavior of the supercell volume during MDM. The oscillations are very noticeable during the first 500−600 ps with amplitude of 3%, and then the oscillations drop to 1% with volume reduction below the average value (78.297 nm^3) during MDM time by 0.5%.

Therefore, the structure was subject to atomic grid reconfiguration and reached the optimal configuration. Structure in Fig. 2, *a* corresponds to optimal supercell configuration with sizes of 3.73 × 5.10 × 4.10 nm. Of course, with tubes number increase in the supercell its volume also increased. Lengths of all tubes are ∼ 4.5 ± 0.2 nm.

Analysis of the supercell density distribution shows its characteristic heterogeneity for both models, i.e. the island structure, while density in Z axis direction significantly changes during supercell passing around in XY plane. Figure 3 shows the maps of graphene/nanotube films density distribution. For the purpose of convenience, the supercells are shown from Z axis position (from the top) and the maps are presented alongside. Abscise axis of the map is X axis of the supercell, ordinate axis is Y axis (measurement units — angstroms). Density measurement units are relative, i.e. the maximum density value is taken as „1“Ṡupercells bodies and regions with maximum density are clearly observed.

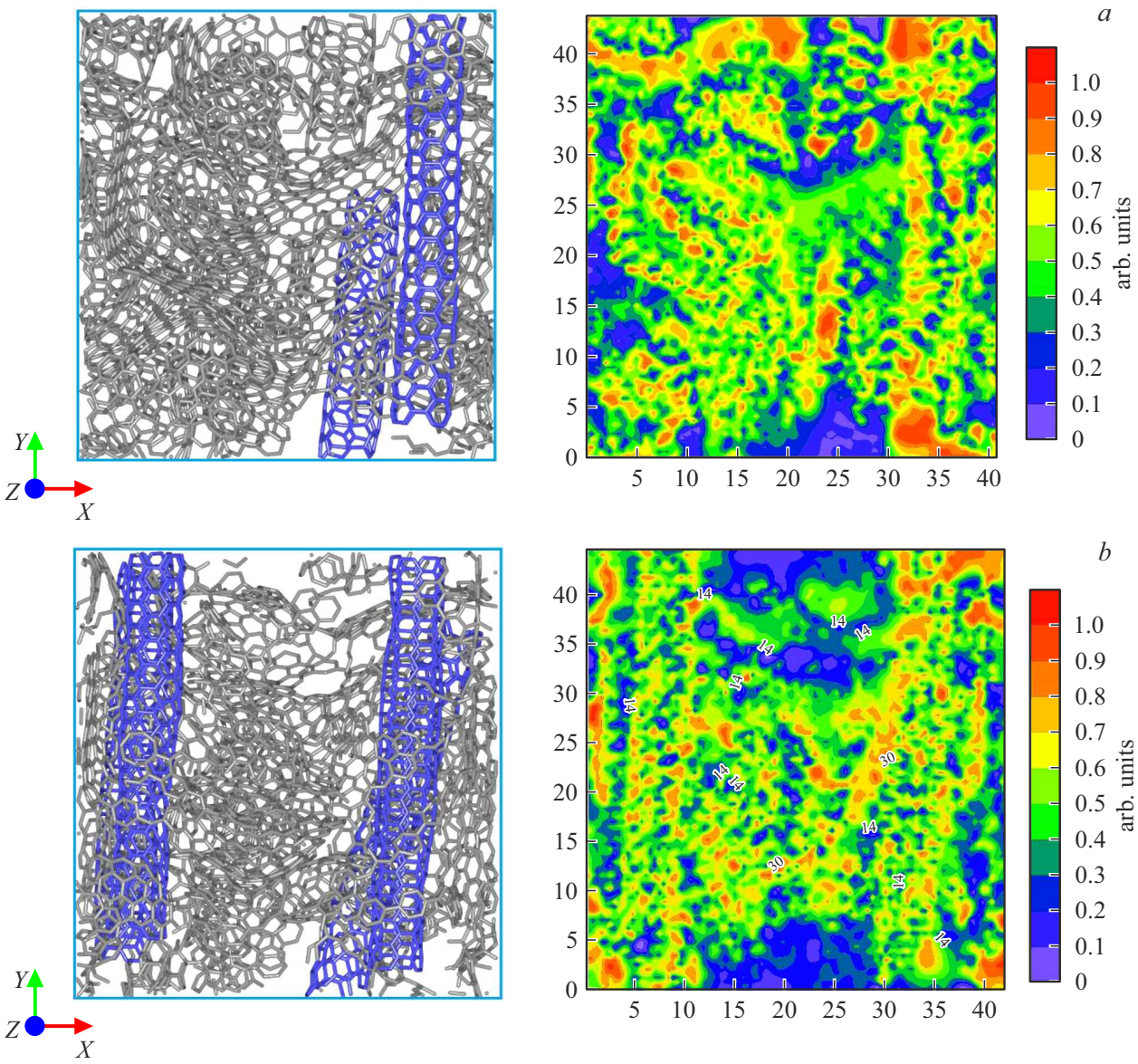

Figure 3. Distribution of density of island structures: (*a*) for model with two nanotubes; (*b*) for model with four nanotubes.

The presented density maps visually demonstrate the island structure of graphene/nanotube films. Density for the first model supercell is 1.143 g/sm^3, density for the second model — 1.108 g/sm^3. Indeed, increase of the tubes in the cell resulted in its loosening, that is seen in Fig. 3, *b*, where bodies became bigger in size.

4. Tunnel contacts in graphene/nanotube films with island structure

As was mentioned above, the thin graphene/nanotube films have a very complex topology and developed structure, where individual fragments contact not only using covalent bonds, but also with Van der Waals interaction. When connecting to electrodes, the tunnel current will be observed between the fragments of Van der Waals interaction, and this current mainly defines electric conductivity of the whole structure. For the models, presented above, one of such contacts is presented in Fig. 4, *a*. These are two supercells of the first model. There is Van der Waals interaction between two tubes at a distance of $\sim 0.3-0.4$ nm (tubes are in the upper part of the figure).

As was mentioned above (see section 2), within the approach, applied for tunnel contacts study, two semi-infinite film fragments without covalent bond are used as electrodes. Schematically it can be presented using example of two tubes the following way: two semi-infinite tubes lay on insulating substrate (for instance, SiO_2), that, in its turn, is located on a silicon substrate, as shown in Fig. 4, *b* for two contacting tubes (12,6). Gate voltage V_g is applied to the bottom layer. The tubes themselves are the left (L) and the

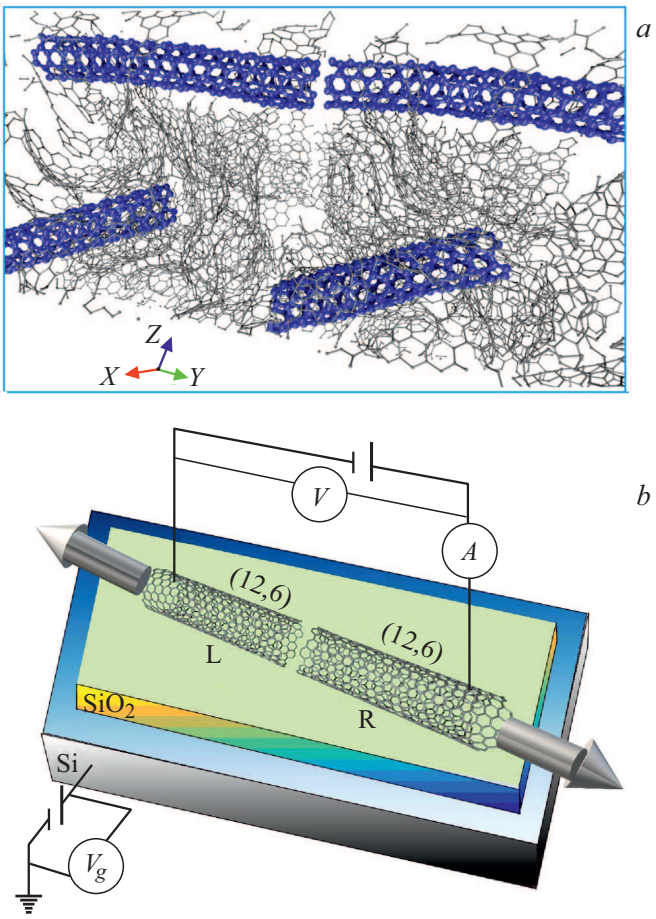

Figure 4. Tunnel contact: (*a*) atomistic model of tunnel contact of two nanotubes as part of the film; (*b*) scheme of tubes connection for tunnel current measurement through the example of tubes (12,6).

right (R) electrodes. Arrows indicate directions of the tubes infinite spreading. As per presented scheme the volt-ampere characteristics (VAC) were calculated for tunnel contacts of the tubes (6,3) and (4,4), which are the fragments of the built models, as well as of tubes (6,5), (12,6) and (16,0). The calculated VAC are shown in Fig. 5, *b*. Diagrams for tubes with metallic nature of conductivity (4,4) and (12,6) are clearly distinguished. They have no zero region, and current appears at small voltages already. At the same time, the linear region of current growth is initially observed, and then it is replaced with a sharp current increase, that is not observed for any of the other examined tubes. I.e. at the certain voltage between electrodes the current transfer between the tubes happens without restriction and quickly increases with the further voltage increase. VAC diagram for contact (16,0)–(16,0) is characterized with a sharp peak of current increase with the further demonstration of negative differential resistance. The further current increase is observed, but current value is significantly less compared to contact of (12,6)–(12,6) and even (4,4)–(4,4) type. Such surge of current value for contact (16,0)–(16,0) can be explained with a regular (non-chiral) structure of atomic grid and the biggest diameter of a body compared to all other examined tubes. The biggest diameter provides the largest amount of contacting atoms of adjacent tubes. The worst characteristics were observed for contacts of tubes of (6,3)–(6,3) and (6,5)–(6,5) type. Both types of tubes are belong to sub-nanometric diameter tubes, therefore the small number of contacting atoms is located in the region on tunnel contact. This results in slow growth of current with voltage increase. And, if slow, but stable increase of current with voltage is observed for contact (6,3)–(6,3), than for contact (6,5)–(6,5) the current growth is replaced with a

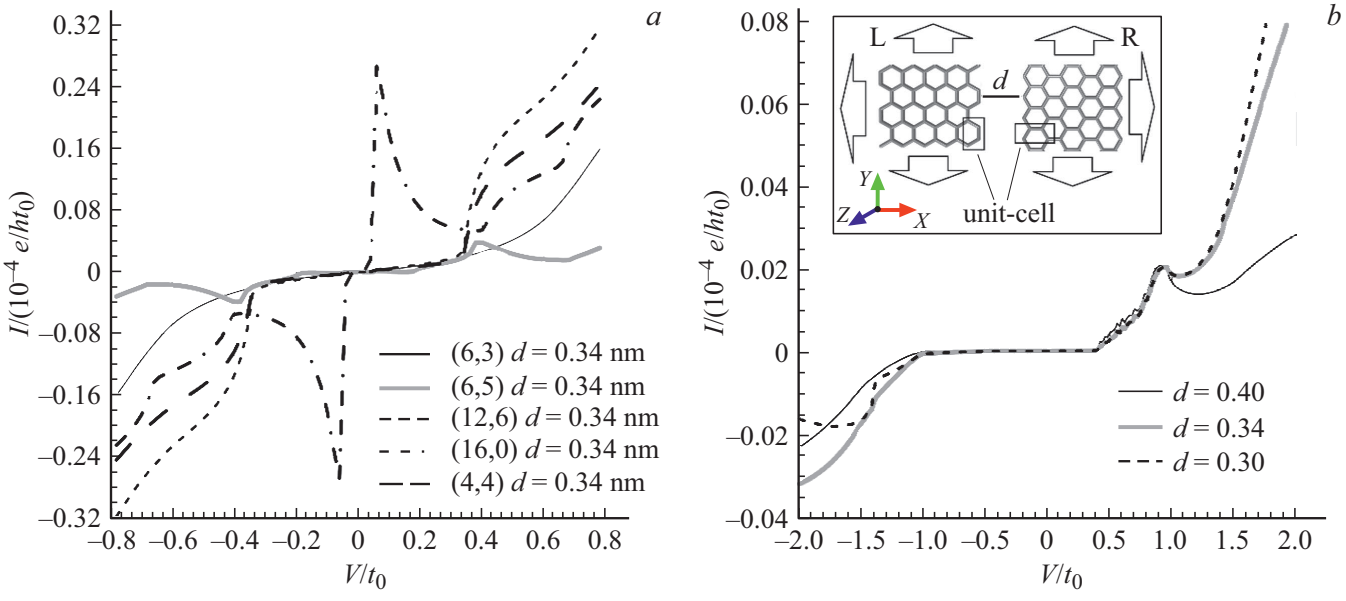

Figure 5. Volt-ampere characteristics at gate voltage $V_g = 0.05t_0$: (*a*) for tunnel contacts between the tubes; (*b*) for tunnel contact between graphene sheets.

negative differential resistance, as for contact (16,0)−(16,0). It can be assumed, that such behavior of VAC for the tubes with semiconductor conductivity type is explained by peculiarities of their band structure. Without a doubt, this topic requires additional significant studies. It should be noted here, that distance d between the tubes was selected different, but considering their chirality to provide the lowest distance between atoms of the adjacent tubes in contact region.

VAC calculations for contact of two semi-infinite graphene sheets with different edges *zigzag* and *armchair*, as shown in insert in Fig. 5, *b*, were also performed. This figure shows the fragments of two graphene sheets, which are infinite in Y direction and semi-infinite in $-X$, X directions. The lattice cells of graphene sheets are indicated with black rectangles. For L-electrode the cell was carried along Y with a step of 2.84 Å and in $-X$ direction — with a step of -2.46 Å, for R-electrode the cell was carried along Y with a step of 2.46 Å and in $+X$ direction — with a step of 2.46 Å. It is seen, that distances between atoms of the adjacent graphene sheets vary over the whole edge along Y axis. This results in slow increase of tunnel current and appearance of voltage interval with negative differential resistance, that narrows with decrease of distance d between graphene sheets. Here, as in the case of the tubes, graphene sheets are electrodes (see Fig. 4, *b*). As expected, VAC curves are not symmetrical.

5. Conclusion

Atomistic models of graphene/nanotube films with covalent and Van der Waals bonds between film fragments are built. It is shown, that thin tubes (4,4) and (6,3), which are part of the film, are covered with a „coating" of graphene sheets and shells, that makes the thin tubes of sub-nanometric diameter energy-stabilized and stable. The created atomistic models of the films demonstrate the explicit island structure, showing strong heterogeneity of density distribution, that is caused by a presence of tubes among graphene fragments, mainly forming an atomic carcass of the film.

Tunnel contacts of two graphene sheets with different topology of contacting edges *zigzag* and *armchair* depending on distance between them, as well as tunnel contacts of the tubes of various chirality (6,3) and (4,4), which are fragments of the built models, as well as tubes (6,5), (12,6) and (16,0), are studied *in silico*. It was revealed, that tunnel contacts of the tubes with semiconductor conductivity type are characterized with a presence of voltage intervals with negative differential resistance in VAC. This is an important moment for the film characteristics, since, as known, 2/3 of all synthesized tubes, as part of the films, are of semiconductor type. Such intervals with negative differential resistance are not observed at all in case of contacts of the tubes with metallic conductivity type. The obtained new knowledge on tunnel contacts of graphene/nanotube films fragments is very important for assessment of electrical conductivity of such films, widely used now in flexible and highly stretchable electronics, as well as planar electronics.

Funding

The work was supported by the grant of the President of the Russian Federation (project No. MK-2289.2021.1.2) and the grant from the Russian Science Foundation (project No. 21-19-00226).

Conflict of interest

The authors declare that they have no conflict of interest.

References

[1] J. Liu, R. Li, H. Li, Y. Li, J. Yi, H. Wang, X. Zhao, P. Liu, J. Guo, L. Liu. New Carbon Mater. **33**, *6*, 481 (2018).
[2] A.Yu. Gerasimenko, A.V. Kuksin, Y.P. Shaman, E.P. Kitsyuk, Y.O. Fedorova, A.V. Sysa, A.A. Pavlov, O.E. Glukhova. Nanomaterials **11**, *8*, 187 (2021).
[3] X. Jia, M. Hofmann, V. Meunier, B.G. Sumpter, J. Campos-Delgado, J.M. Romo-Herrera, H. Son, Y.P. Hsieh, A. Reina, J. Kong, M. Terrones, M.S. Dresselhaus. Science **323**, 5922, 1701 (2009).
[4] C. Jin, H. Lan, L. Peng, K. Suenaga, S. Iijima. Phys. Rev. Lett. **102**, *20*, 205501 (2009).
[5] A. Chuvilin, J.C. Meyer, G. Algara-Siller, U. Kaiser. New J. Phys. **11**, *8*, 083019 (2009).
[6] Y. He, H. Dong, T. Li, C. Wang, W. Shao, Y. Zhang, L. Jiang, W. Hu. Appl. Phys. Lett. **97**, *13*, 133301 (2010).
[7] H.M. Wang, Z. Zheng, Y.Y. Wang, J.J. Qiu, Z.B. Guo, Z.X. Shen, T.Yu. Appl. Phys. Lett. **96**, *2*, 023106 (2010).
[8] D.A. Ryndyk, J. Bundesmann, M.H. Lin, K. Richter. Phys. Rev. B **86**, *19*, 195425 (2012).
[9] A.M. Ionescu, H. Riel. Nature **479**, *7373*, 329 (2011).
[10] A.D. Franklin, Z. Chen. Nature Nanotechnol. **5**, *12*, 858 (2010).
[11] H. Alhassen, V. Antony, A. Ghanem, M.M.A. Yajadda, Z.J. Han, K.K. Ostrikov. Chirality **26**, *11*, 683 (2014).
[12] S. Yick, M.M.A. Yajadda, A. Bendavid, Z.J. Han, K.K. Ostrikov. Appl. Phys. Lett. **102**, *23*, 233111 (2013).
[13] A. Salehi-Khojin, F. Khalili-Araghi, M.A. Kuroda, K.Y. Lin, J.P. Leburton, R.I. Masel. ACS Nano **5**, *1*, 153 (2011).
[14] M.M. Aghili Yajadda. J. Phys. Chem. C **120**, *7*, 3646 (2016).
[15] C. Berthod, T. Giamarchi. Phys. Rev. B **84**, *15*, 155414 (2011).
[16] Mizar [software]. URL: http://nanokvazar.ru, date of access: 10.03.2021.
[17] V.L. Katkov, V.A. Osipov. Pis'ma v ZhETF **98**, *11*, 782 (2013) (in Russian).
[18] B. Hourahine, B. Aradi, V. Blum, F. Bonafé, A. Buccheri, C. Camacho, C. Cevallos, M.Y. Deshaye, T. Dumitrică, A. Dominguez, S. Ehlert, M. Elstner, T. van der Heide, J. Hermann, S. Irle, J.J. Kranz, C. Köhler, T. Kowalczyk, T. Kubař, I.S. Lee, V. Lutsker, R.J. Maurer, S.K. Min, I. Mitchell, C. Negre, T.A. Niehaus, A.M.N. Niklasson, A.J. Page, A. Pecchia, G. Penazzi, M.P. Persson, J. Řezáč, C.G. Sánchez, M. Sternberg, M. Stöhr, F. Stuckenberg, A. Tkatchenko, V.W.Z. Yu, T. Frauenheim. J. Chem. Phys. **152**, *12*, 124101 (2020).